PAPER

Electropolymerization using binuclear nickel(II) *Schiff* base complexes bearing N$_4$O$_4$ donors as supramolecular building blocks†

Cibely S. Martin, Wesley B. S. Machini and Marcos F. S. Teixeira*

The supramolecular building blocks from a nickel(II) *bisalphen*-type complex have been reported. The conjugations through the bridge provide flexibility of the monomer in the electropolymerization stage. Thus, different structures can be obtained with the variation of electrochemical parameters used in the electropolymerization. The structural characterization and the electrochemical behavior in aqueous solution was also evaluated, which demonstrated that the electropolymerization mechanism was similar to that observed for the classical *salen* polymers, but the molecular organization onto the conductor substrate was different. The supramolecular structure of the polymeric film allows observation of the Ni^I/Ni^{II} and Ni^{II}/Ni^{III} redox couples by differential pulse voltammetry. Thus, the comproportionation constant and Gibbs energy were calculated for the Ni^I/Ni^{II} redox couple. These characteristics make these polymers versatile materials in the field of supramolecular chemistry and materials science, in particular in applications as sensors, in electrocatalysts and for energy storage.

Introduction

The *salen* ligands play an important role in the development of sensors, not only due to the variety of transition metals that can be incorporated, but also the variety of ligand derivatives from classical *salen*.[1–3] In addition, the *salen* polymers containing transition metal complexes are of special interest, given their ease of preparation by electropolymerization as well as their conducting character in aqueous solution.[4–9] Among the principal metal–*salen* complexes, binuclear complexes are currently of great interest in the field of supramolecular chemistry and materials science[10–12], and have shown in some cases an unusual behavior, ascribed to conformational mobility. Thus, the development of new polymers with binuclear complexes has raised interest in applications such as electrochemical,[13,14] chemiluminescent[15,16] and optical[17] sensors. The properties of metal complex derivatives from bis(*salen*) can be similar to classical *salen* complexes, since the bis(*salen*) complexes should have two independent moieties of *salen* ligands.[18] In particular, the 3,3′-diaminobenzidine framework offers versatile molecular building blocks. Supramolecular building blocks can be obtained from derivatives of bis(*salen*) complexes in solution.[19,20] Curreli *et al.*[19] described the synthesis of various bis(*salen*) complexes and showed the supramolecular assembly formation by combining two of these complexes with a ditopic

ligand. On the other hand, the complexes derived from bis(*salen*) can be applied to thin film formation. Byrd *et al.*[21] reported obtaining polymeric films using a layer-by-layer method, where they showed that robust homogeneous films occur due to strong coordination between the metal and the ligands.

However, the polymeric film obtained from nickel-*bisalphen* [Ni$_2$(*bisalphen*)] by electropolymerization was firstly reported by Aubert *et al.*[18] In their study, the polymer was formed by a potential applied in a saturated solution of [Ni$_2$(*bisalphen*)] in acetonitrile, due to low solubility. The authors evaluated that charge was necessary for formation of the polymer, and concluded that the polymeric formation was related to the amount of metallic cation present in the monomeric structure and the potential to over-oxidize the polymer.[18] Thus, the present paper describes a complementary and comparative study of the electropolymerization stage, and the electrochemical behavior and morphological features were realized for the [Ni$_2$(*bisalphen*)] complex (Scheme 1) in tetrahydrofuran. Also, the comproportionation constant and Gibbs energy were calculated.

Experimental

Apparatus

All voltammetric measurements were carried out in a 25 mL thermostatic glass cell containing three-electrodes: a platinum electrode coated with a thin film of nickel–*bisalphen* polymer as the working electrode (surface area of 0.071 cm^2), a saturated calomel electrode (SCE) as the reference, and a platinum auxiliary electrode. The electrochemical measurements were

Faculty of Science and Technology, São Paulo State University, Roberto Simonsen St, 305, 19060-900, Presidente Prudente, São Paulo, Brazil. E-mail: funcao@fct.unesp.br
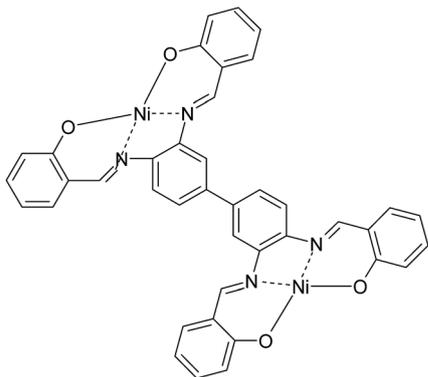
Scheme 1 Molecular structure of the N,N',N'',N'''-tetrabis(salicylidene)-3,3',4,4'-biphenylenetetraimino of bis-nickel(II).

conducted with a μ-Autolab type III (Eco Chimie) connected to a microcomputer and controlled by GPES 4.9 software. The Raman spectra were obtained using a Renishaw Raman spectrometer with a laser at an excitation wavelength of 663 nm. The optical microscopy images were obtained using a Leica optic microscope, DMRX model (eyepiece lens of 10× and objective lenses of 50×) for the polymer formed on a platinum surface. The scanning electron microscopy (SEM) images were obtained using a Carls Zeiss microscope, model EVO LS15, and atomic force microscopy (AFM) images, using a Nanosurf microscope model Easyscan 2, tapping mode (intermittent contact) and a resolution of 512 dots per line, were obtained for the polymer formed on ITO glass.

Synthesis of [Ni₂(*bisalphen*)]

The *bisalphen* (N,N',N'',N'''-tetrabis-(salicylidene)-3,3',4,4'-biphenylenetetraimino) ligand was prepared as previously described in the literature.[18] The *bisalphen* ligand (1.58 mmol) was dissolved in ethanol (50 mL) and slowly added dropwise over a suspension of nickel(II) acetate (3.16 mmol) in the same solvent (50 mL). The solution was refluxed for 36 hours (at 60 °C), and the red precipitate was filtered and recrystallized from methanol. The obtained product was stored under vacuum at room temperature. FTIR (ν cm^{-1}): 2651 –OH$_{ph}$, 1608 C=C, 1527 C=N, 1362 >C–O$_{ph}$, 1023 breathing ring, 765 Ni–O. UV-vis (nm): 262 ($\pi \rightarrow \pi^*$), 312 ($\pi \rightarrow \pi^*$), 388 (n $\rightarrow \pi^*$), 495 (MLCT).

Preparation of metallo-supramolecular polymer

The polymer film on a conductive surface was obtained by electropolymerization of the [Ni₂(*bisalphen*)] complex in THF/0.1 mol L^{-1} TBAP (under a nitrogen atmosphere) by cyclic voltammetry between 0.0 and 1.4 V versus SCE. The scan rate (15 mV s^{-1} to 150 mV s^{-1}), potential cycle number (3 to 5 cycles) and the monomer concentration (0.1 mmol L^{-1} to 1.0 mmol L^{-1}) were evaluated for polymeric film formation. Visual inspection of the platinum surface showed the deposition of a dark orange film.

Electrochemical behavior

In each electropolymerization study, the electrochemical behavior was investigated in 0.5 mol L^{-1} KCl solution by differential pulse voltammetry (pulse of 50 mV and scan rate of 5 mV s^{-1}). All measurements were carried out with a continuous flow of nitrogen gas. The voltammograms were used to calculate the electroactive surface coverage Γ (mol cm^{-2}), ensuring that the oxidation/reduction processes could occur on the whole film. The influence of the anions (Cl$^-$, ClO$_4^-$, NO$_3^-$, SO$_4^{2-}$) and cations (Li$^+$, Na$^+$, K$^+$, Mg^{2+}, Ca^{2+}, Ba^{2+}) was studied in an aqueous solution of 0.5 mol L^{-1} concentration. The pH effect using a universal buffer solution (1.0 to 10.0) containing 0.5 mol L^{-1} KCl as the supporting electrolyte was also investigated.

Results and discussion

[Ni₂(*bisalphen*)] film formation by cyclic voltammetry

Initially, the poly[Ni₂(*bisalphen*)] was obtained in THF/0.1 mol L^{-1} TBAP by cyclic voltammetry between 0.0 and 1.4 V versus SCE at 100 mV s^{-1} with 15 polymerization cycles (Fig. 1). The fast mechanism of electropolymerization was similar to the mechanism observed for classical *salen*,[22,23] since the *bisalphen* complexes should have two independent *salen* units, due to weak conjugation through the bridge.[18,24] However, two important steps were observed for poly[Ni₂(*bisalphen*)] formation in THF solvent, as illustrated in Fig. 1 (insert). The first potential cycle showed an increase in anodic current at 1.0 V versus SCE, ascribed to the radical formation, in accordance with studies by Aubert et al.[18] In the first potential cycle, one cathodic peak at 0.69 V versus SCE was also observed, and was ascribed to the reduction of Ni^{III} to Ni^{II} present on the polymeric structure formed.[25] The second potential cycle showed one redox couple (E_{pa} = 0.87 V and E_{pc} = 0.67 V vs. SCE), ascribed to the redox couple Ni^{II}/Ni^{III} of the polymeric film. The other potential cycles were applied to keep the growth of the polymer on the electrode surface. The current responses to subsequent potential cycles decrease progressively after four cycles. This can be ascribed to the formation of an electroactive film which impedes the
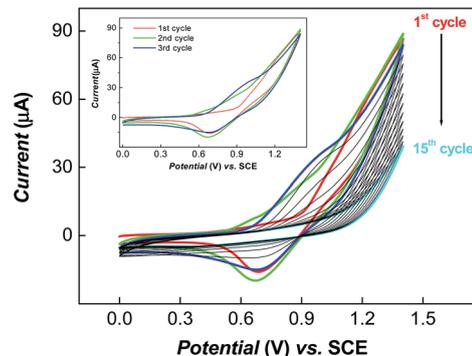

Fig. 1 Cyclic voltammogram of the electropolymerization stage to 1.0 mmol L^{-1} of the [Ni₂(*bisalphen*)] complex in THF/0.1 mol L^{-1} TBAP using a platinum electrode applying 15 potential cycles between 0.0 V and 1.4 V vs. SCE at 100 mV s^{-1}. Insert: cyclic voltammogram for the first three potential cycles of the electropolymerization.

diffusion of free monomers to the electrode surface and consequently decreases the oxidation of additional monomers for polymer formation.

The mechanism of the electro-oxidative polymerization of the complex still remains unclear. However, according to the previously reported data on the anodic oxidation of metal–*salen* complexes,[4–7,26] the polymerization corresponds to the electron transfer from predominantly ligand-centered orbitals. The results corroborate the hypothesis that the model for the structure of poly(metal–*Schiff*) on the electrode surface is the generation of stacked polymer complexes (charge transfer complexes) formed due to the donor–acceptor interaction between the ligand of one monomer fragment and the metal center of another. Thus the supramolecular aggregates are not formed without oxidation of the central metal and/or correct orientation of the ligand and the metal center. Thus, the supramolecular blocks are dependent on the interaction between the d-bonding orbitals of the metal centers with the π orbitals of aromatic rings of the adjacent molecules.

The difference in the electropolymerization profile and stability of the polymer film formed can be related to the physical and chemical properties of the solvent used in the electropolymerization stage. The solvents used in this study were THF and DMF. This selection was based on the high solubility of the complex in these solvents. In DMF solvent, the formation of the polymeric film on the electrode surface was not observed. This solvent has a high viscosity (0.802 cP)[25] and directly influences the process of diffusion of the monomer species to the electrode surface. The dipole moment can be related to the stability of radical cations in solution. With the lower dipole moment (1.75μ to THF), the stability of radical cations in solution is higher; as a result, a large amount of radical–radical attack may occur, favoring the formation of large polymer chains. This way, the poly[Ni_2(*bisalphen*)] formed in THF showed different voltammetric profiles in the electropolymerization stage and better stability in aqueous solution.

The studies by Vilas-Boas and coworkers[6,26] concluded that the poly(*salen*) behaves like a polyphenylene compound, where the metal ion acts as a bridge between biphenylene moieties. Thus, the polymeric structure is formed by interaction of the dπ molecular orbital of the metal center with the π molecular orbital of the aromatic ring of the adjacent monomers. Consequently, the metal cation does contribute to the π-delocalized system responsible for the charge conjugation.[6,26] The same behavior was observed in poly[Ni_2(*bisalphen*)], but the structural organization was not uniform like in the polymers formed from classic *salen* complexes. Due to morphology changes of the monomer resulting from weak conjugation through the bridge, the polymeric structures were formed in clusters, and the blocks are formed from supramolecular structures. The schematic comparison of the film structures of *salen* and *bisalphen* are illustrated in Scheme 2.

The images from optical microscopy (Fig. 2A) and scanning electron microscopy (SEM) (Fig. 2B), obtained on the surface of platinum coated with the poly[Ni_2(*bisalphen*)], show many clusters along the polymeric film, indicating that the polymer film was formed from supramolecular blocks.

Influence of electrochemical parameters

The formation of the polymeric film can be influenced by electrochemical parameters used in the electropolymerization stage, such as potential cycle number and scan rate. The monomer concentration can also influence the polymer formation. The number of potential cycles applied in the electropolymerization stage is related to the amount and/or size of the supramolecular block structures formed on the conductive surface. This study was carried out with 1.0 mmol L^{-1} [Ni_2(*bisalphen*)] in THF/0.1 mol L^{-1} TBAP varying the number of potential cycles from 3 to 50. All polymeric films were obtained between 0.0 V and 1.4 V *versus* SCE at 100 mV s^{-1}. The cyclic voltammograms obtained in the electropolymerization stage showed the same behavior, where the first two potential cycles were crucial for the polymeric formation. However, the polymeric film growth was non-linear to the number of applied cycles (ESI – S1†). Adsorbed molecules at the electrode surface are described by the surface coverage and the peak current becomes linear to concentration in the thin layer. In this study, the peak current of the electrode coated with poly[Ni_2(*bisalphen*)] depends sigmoidally on the number of layers deposited. This characteristic can be ascribed to the fact that the building of the supramolecular blocks is dependent on the molecular structure. Thus, due to weak conjugation through the bridge and the number of aromatic rings present in the monomeric structure, the *bisalphen*-type complexes show great structural flexibility in the formation of polymeric films through to supramolecular building blocks. The blocks can also be observed in the image obtained from AFM, which shows big structures of nanometer size (Fig. 3).

Due to these properties, the scan rate applied in the electropolymerization can influence the polymer formation onto the electrode surface. In the literature, Li and coworkers[27] described the scan rate effect (5 mV s^{-1} to 150 mV s^{-1}) in the anodic polymerization of Ni–*salen* complexes. Their studies proved that the growth rate of polymeric films increases at low scan rate values, where the best results were obtained at 20 mV s^{-1}. High scan rates directly influence the kinetic diffusion of the monomer to the electrode surface causing, consequently, a decrease in the amount of polymer film formed.[27] On the other hand, the surface coverage of [Ni_2(*bisalphen*)] was non-linear to the scan rate used in the electropolymerization stage (ESI – S2†). This can be ascribed to the structural flexibility of the *bisalphen* ligand. In this way, the subsequent studies were carried out at moderate scan rates and potential cycles to try to establish a more uniform structure of the polymer.

The monomer concentration was also evaluated to understand the electropolymerization stage. The study was performed in THF/0.1 mol L^{-1} TBAP solution, at a monomer concentration in the range 0.05 mmol L^{-1} to 1.0 mmol L^{-1}. Concentrations higher than 1.0 mmol L^{-1} were not analyzed due the solubility of the monomer in the solvent. An increase of surface coverage ($\Gamma = $ mol cm^{-2}) with an increase of monomer concentration was observed, as shown in Fig. 4.
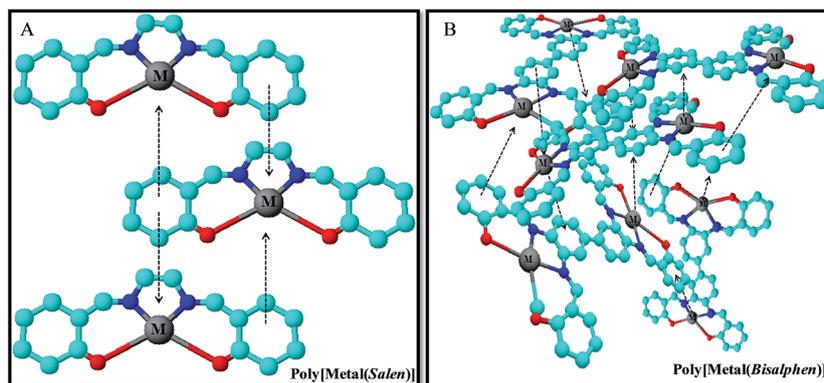
Scheme 2 Comparison of the polymeric film structure of (a) metal–*salen* and (b) metal–*bisalphen* complexes. Colors: cyan = carbon; blue = nitrogen; red = oxygen; gray = transition metal.

A monomer concentration of 0.5 mmol L^{-1} was sufficient to achieve maximum surface coverage of the poly[Ni$_2$(*bisalphen*)] onto the platinum surface. Besides, the high concentration of the Ni$_2$(*bisalphen*) complex causes agglomerate formation in solution, which decreases the radical cation formation, and consequently decreases the amount of film formed in each scanning cycle. On the other hand, moderate concentrations allow the electrogeneration of the radical cations and the formation of thicker films.

Electrochemical behavior of poly[Ni$_2$(*bisalphen*)] in aqueous solution

The electrochemical behavior of poly[Ni$_2$(*bisalphen*)] in aqueous solution was evaluated in 0.5 mol L^{-1} KCl solution at 5 mV s^{-1} by differential pulse voltammetry between −0.70 V and 0.80 V *vs.* SCE with 50 mV pulses. Fig. 5 shows the voltammograms obtained on the platinum surface coated with the poly-[Ni$_2$(*bisalphen*)] for the anodic process. The voltammetric profile for the poly[Ni$_2$(*bisalphen*)] formed after 3 potential cycles shows just one redox process ($E_{pa}^{(peak\ I)} = -183$ mV) ascribed to the Ni^I/Ni^{II} redox couple. On the other hand, the poly-[Ni$_2$(*bisalphen*)] formed with 15 cycles shows three redox processes. Peaks I and II ($E_{pa}^{(peak\ I)} = -371$ mV and $E_{pa}^{(peak\ II)} =$
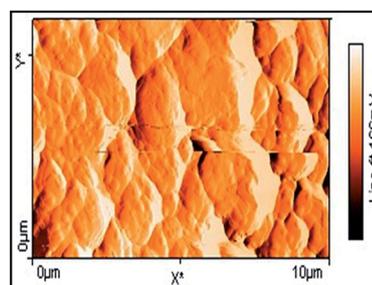
Fig. 3 AFM image of the surface of ITO coated with the poly [Ni$_2$(*bisalphen*)].

−42 mV) can be ascribed to the Ni^I/Ni^{II} redox couple and peak III ($E_{pa}^{(peak\ III)} = 600$ mV) can be ascribed to Ni^{II}/Ni^{III}.

This behavior can be ascribed to orbital overlap driving the molecular organization of the polymeric film, providing two oxidation potentials for the same oxidation state of the metal center, and may be associated with the comproportionation effect. An important observation is that the larger the supramolecular blocks formed in the electropolymerization stage, the greater the comproportionation effect. Thus, more clustered structures provide a greater overlap of orbitals and
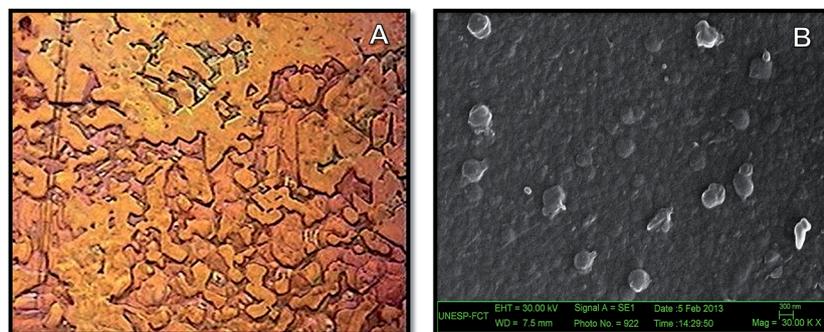

Fig. 2 The images from (A) optical microscopy (magnification – 500×), obtained on the surface of platinum coated with the poly[Ni$_2$(*bisalphen*)] and (B) scanning electron microscopy (SEM) (magnification – 30 000×), obtained on the surface of ITO coated with the poly[Ni$_2$(*bisalphen*)]. The polymer was formed under the same conditions for both surfaces.
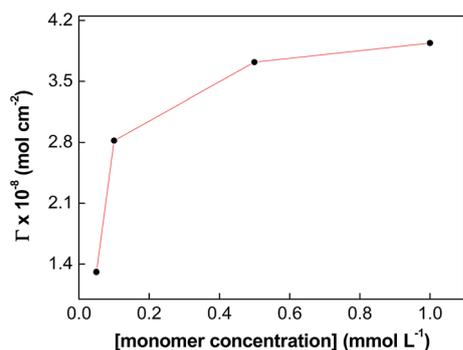
Fig. 4 Surface coverage values (mol cm^{-2}) calculated for poly-[Ni$_2$(*bisalphen*)] in aqueous solution as a function of the monomer concentration used in the electropolymerization stage.
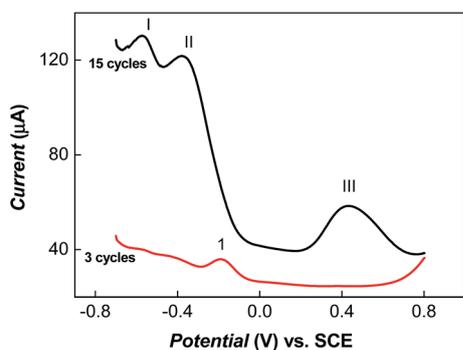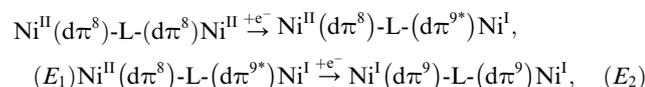

Fig. 5 Differential pulse voltammograms of the poly[Ni$_2$(*bisalphen*)] modified electrode formed with 3 and 15 potential cycles. The electrochemical behavior was investigated in 0.5 mol L^{-1} KCl solution in the absence of oxygen by differential pulse voltammetry (pulses of 50 mV and scan rate of 5 mV s^{-1}).

consequently a greater possibility of electronic transfer processes occurring from the polymeric film to the electrode surface. This electronic communication is generated by overlapping dπ orbitals of the metallic center with π orbitals of the ligand, making the unpaired electron of the metal act as an oscillating load during the redox process. Whereas in a mechanism involving two electrochemical steps, the binuclear supramolecular complex may be represented by:

$$Ni^{II}(d\pi^8)\text{-}L\text{-}(d\pi^8)Ni^{II} \xrightarrow{+e^-} Ni^{II}(d\pi^8)\text{-}L\text{-}(d\pi^{9*})Ni^{I},$$

$$(E_1)Ni^{II}(d\pi^8)\text{-}L\text{-}(d\pi^{9*})Ni^{I} \xrightarrow{+e^-} Ni^{I}(d\pi^9)\text{-}L\text{-}(d\pi^9)Ni^{I}, \quad (E_2)$$

where "*" represents the unpaired electron which gives rise to the electronic delocalization during the redox process, L is the ligand and E_1 and E_2 are reduction potentials.

Due to the increased possibility of the application of the electrocatalytic effect caused by the comproportionation effect, the parameters of the comproportionation effect (K_c – comproportionation constant and ΔG° – Gibbs energy) were calculated for a platinum surface coated with the poly[Ni$_2$(*bisalphen*)]. The electropolymerization was carried out at 1.0 mmol L^{-1} of the monomer in THF/0.1 mol L^{-1} TBAP applying 15 potential cycles at 50 mV s^{-1}, and the

electrochemical behavior was obtained in 0.5 mol L^{-1} KCl solution at 5 mV s^{-1} (Fig. 5). The comproportionation constant can be calculated by eqn 1:[28,29]

$$K_c = \exp\left(\frac{\Delta E_{1/2}}{25.69 \text{ mV}}\right) \quad (1)$$

where $E_{1/2}$ is measured in mV. This equation can be applied when the redox process involves only one electron. Thus, K_c was calculated for the Ni^I/Ni^{II} redox couple. The calculations showed a comproportionation constant of 8.86 × 10^3 in KCl solution, ascribed to moderate system coupling.[30,31] This comproportionation constant value is in agreement with the formation of the polymeric film by interaction and not by effective bonding.

This way, the Gibbs free energy can be calculated by:

$$\Delta G^\circ = -RT \ln K_c \quad (2)$$

Through this relation, the electronic transitions can display an exergonic ($\Delta G^\circ < 0$, thermodynamically favorable) or endergonic ($\Delta G^\circ > 0$, thermodynamically unfavorable) character, where donor species or recipients of electrons that make up the system must be chemically or electrochemically distinct. This difference is necessary for a change in energy during the electron transfer process to occur. Thus, in the presence of potassium ions in solution, the poly[Ni$_2$(*bisalphen*)] presented a thermodynamically favorable system with ΔG° equivalent to -22.52 kJ mol^{-1}.

Counterion effect

A repulsive force must also be present in the poly[Ni$_2$(*bisalphen*)] structure, which would impose a flexible structure. In this way, the movement of species from solution into the film is necessary and can be associated with the polymer charge transfer.[32] Therefore, the counter ion effect is needed to understand the stability of poly[Ni$_2$(*bisalphen*)] in aqueous solution. The platinum coated with the poly[Ni$_2$(*bisalphen*)] was evaluated in various supporting electrolytes with different anions such as Cl$^-$, NO$_3^-$, ClO$_4^-$, and HSO$_4^-$, but with a similar cation (sodium ion) concentration of 0.5 mol L^{-1}. In the same way, the influence of different cations (Li$^+$, Na$^+$, K$^+$, Mg^{2+}, Ca^{2+} and Ba^{2+}) on electrochemical behavior of the polymeric film was studied. The solutions were prepared with a similar anion (chloride ion) concentration of 0.5 mol L^{-1}. The strong dependence on the anion present in solution was observed for the Ni^{II}/Ni^{III} redox potential (see Fig. 6). Although there has been an influence on the comproportionation effect, the potential of Ni(I) was almost always the same. It can be seen that the maximum current potential in the presence of various anions has the same potential level. The average peak potential for Ni(I) is shown by the dotted line in Fig. 6.

The anion influence on the Ni^{II}/Ni^{III} redox couple may be related to stabilization of the positive charge of the polymer, when Ni(III) is formed by the anodic scan. The results indicate that the anion in solution induces the redox couple in the following order: Cl$^-$ (0.429 V) < HSO$_4^-$ (0.544 V) < NO$_3^-$ (0.604 V) < ClO$_4^-$ (0.642 V) and these are shifted to more anodic values

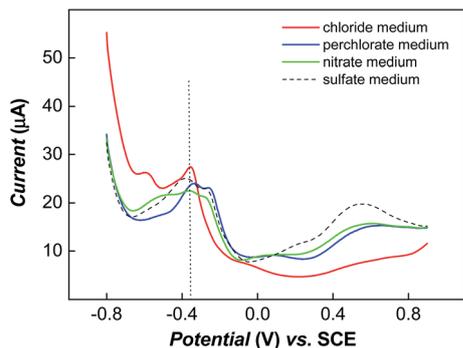**Fig. 6** Differential pulse voltammogram of the poly[Ni$_2$(*bisalphen*)] modified electrode in the presence of different anions (ClO$_4^-$, Cl$^-$, NO$_3^-$, HSO$_4^-$) at 0.5 mol L^{-1} (pulse = 50 mV; scan rate = 5 mV s^{-1}).

with the increase in ionic radius[33] of the anion. This same behavior was observed for polymers derived from classic *salen* polymers.[4]

In the same way, the cation influence on the Ni^I/Ni^{II} redox couple (ESI – S3†) may be related to stabilization of the negative charge of the polymer, when Ni(I) is formed by the cathodic scan. We can conclude that anions influenced the redox processes in Ni(II)/Ni(III) and cations influenced the redox processes in Ni(I)/Ni(II), proving the relationship between the formal charge generated in the processes of oxidation and reduction, and the need to balance the charge of the complex ion.

pH effect

The pH study was conducted in a universal buffer containing KCl 0.5 mol L^{-1} as the supporting electrolyte. The pH range measured was 1.0 to 8.0. Two distinct regions were observed for the redox processes as a function of pH, where for pH values lower than 4.0, a strong dependence on more negative potentials was observed, and only the redox processes ascribed to the Ni^I/Ni^{II} redox couple can be observed (Fig. 7).

This profile change can be related to the hydrogen ion concentration of the medium. The higher the H$^+$ concentration of the medium, the greater the difficulty for the Ni^{II}/Ni^{III} redox

process to occur, because the polymer isn't stable in the presence of positive charge, which is consistent with studies of the counter ion. Thus, at low pH values, the Ni^I/Ni^{II} redox process is favored. On the other hand, for higher pH values (above 5.0) the Ni^I/Ni^{II} and Ni^{II}/Ni^{III} redox processes were clearly observed (Fig. 8). This can be ascribed to the increased concentration of the hydroxyl ions in the medium, which stabilize the polymer when the positive charge is formed from the oxidation of Ni^{II} to Ni^{III}. However, at pH 8.0 possible formation of nickel(II) hydroxide (Ni(OH)$_2$) in the polymeric film may occur,[34] and consequently just one redox process was observed (−0.40 V).

Structural characterization by Raman spectroscopy

The poly[Ni$_2$(*bisalphen*)] obtained on the platinum surface was analyzed by Raman spectroscopy. Fig. 9 shows the Raman spectra (excitation 633 nm) obtained for both poly-[Ni$_2$(*bisalphen*)] and the [Ni$_2$(*bisalphen*)] solid monomer, which show similar spectra. This characteristic indicates that the structural conformation of the polymer did not alter the main structure of the monomer, where the increased intensity of peaks can be ascribed to clusters generated and as a result of the stretching magnification of the signal at certain frequencies.[35]

When comparing the Raman spectra of poly[Ni$_2$(*bisalphen*)] and [Ni$_2$(*bisalphen*)], a shift of bond frequency to lower values is observed. This change can be ascribed to the interaction between the monomers present in each layer of the polymer. The principal changes were observed for C=C (1576 cm^{-1} → 1583 cm^{-1}), C=N (1518 cm^{-1} → 1531 cm^{-1}) and C–O$_{ph}$ (1277 cm^{-1} → 1281 cm^{-1}) stretching, which confirm formation of the polymer by the interaction of aromatic rings and the coordination center (N$_2$O$_2$) of the *Schiff* ligand.[4,6,26] The frequency shift and intensity decrease of the C–H out-of-plane deformation (1365 cm^{-1} → 1388 cm^{-1}) was also observed. This can be ascribed to a decrease of vibration out-of-plane due to the formation of layers (molecular columns). In addition, a new band at 931 cm^{-1} ascribed to ring-breathing was observed only in the poly[Ni$_2$(*bisalphen*)] spectrum, which may be associated with cluster vibration.
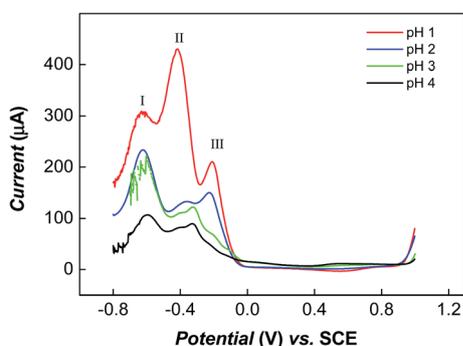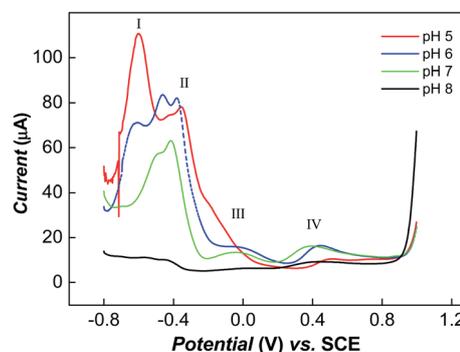

Fig. 7 Differential pulse voltammogram of the poly[Ni$_2$(*bisalphen*)] modified electrode evaluated in a universal buffer with 0.5 mol L^{-1} KCl solution as the supporting electrolyte between pH 1.0 and 4.0.

Fig. 8 Differential pulse voltammogram of the poly[Ni$_2$(*bisalphen*)] modified electrode evaluated in a universal buffer with 0.5 mol L^{-1} KCl solution as the supporting electrolyte between pH 5.0 and 8.0.

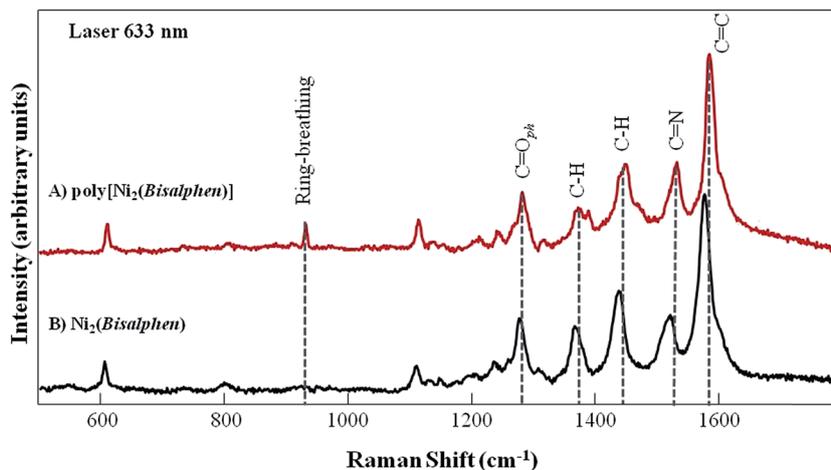**Fig. 9** Raman spectra for (A) poly[Ni_2(*bisalphen*)] on the platinum electrode surface and (B) the [Ni_2(*bisalphen*)] solid monomer (laser: 633 nm).

Conclusion

The poly[Ni_2(*bisalphen*)] formation by electropolymerization is directly influenced by the solvent, which keeps the radical cation in solution for reaction propagation. The supramolecular building blocks are formed by interaction between the metal cation and aromatic rings, similar to the classical *salen* polymers. However, the weak conjugation through the bridge allows the formation of cluster structures. Thus, the polymeric film showed supramolecular blocks, which have characteristics of their monomer units. These characteristics make these polymers versatile materials, in particular in applications such as sensors, in electrocatalysts and in energy storage systems.

Author contributions

The manuscript was written with contributions from all authors.

Funding sources

Conflict of interest

The authors declare no competing financial interest.

Acknowledgements

References

1 P. G. Cozzi, *Chem. Soc. Rev.*, 2004, **33**, 410–421.
2 N. S. Venkataramanan, G. Kuppuraj and S. Rajagopal, *Coord. Chem. Rev.*, 2005, **249**, 1249–1268.
3 A. Zulauf, M. Mellah, X. A. Hong and E. Schulz, *Dalton Trans.*, 2010, **39**, 6911–6935.
4 T. R. L. Dadamos and M. F. S. Teixeira, *Electrochim. Acta*, 2009, **54**, 4552–4558.
5 C. S. Martin, T. R. L. Dadamos and M. F. S. Teixeira, *Sens. Actuators, B*, 2012, **175**, 111–117.
6 M. Vilas-Boas, C. Freire, B. de Castro, P. A. Christensen and A. R. Hillman, *Chem.–Eur. J.*, 2001, **7**, 139–150.
7 M. Vilas-Boas, I. C. Santos, M. J. Henderson, C. Freire, A. R. Hillman and E. Vieil, *Langmuir*, 2003, **19**, 7460–7468.
8 M. Vilas-Boas, C. Freire, B. de Castro and A. R. Hillman, *J. Phys. Chem. B*, 1998, **102**, 8533–8540.
9 C. E. Dahm, D. G. Peters and J. Simonet, *J. Electroanal. Chem.*, 1996, **410**, 163–171.
10 P. G. Cozzi, *Angew. Chem., Int. Ed.*, 2003, **42**, 2895–2898.
11 M. Holbach, X. L. Zheng, C. Burd, C. W. Jones and M. Weck, *J. Org. Chem.*, 2006, **71**, 2903–2906.
12 A. J. Gallant and M. J. MacLachlan, *Angew. Chem., Int. Ed.*, 2003, **42**, 5307–5310.
13 M. Y. Wang, X. Y. Xu and J. Gao, *J. Appl. Electrochem.*, 2007, **37**, 705–710.
14 I. R. W. Z. de Oliveira, A. Neves and I. C. Vieira, *Sens. Actuators, B*, 2008, **129**, 424–430.
15 Y. Zhou, Y. Xiao and X. H. Qian, *Tetrahedron Lett.*, 2008, **49**, 3380–3384.
16 D. H. Lee, S. Y. Kim and J. I. Hong, *Angew. Chem., Int. Ed.*, 2004, **43**, 4777–4780.
17 W. Zhang, E. Rozniecka, E. Malinowska, P. Parzuchowski and M. E. Meyerhoff, *Anal. Chem.*, 2002, **74**, 4548–4557.
18 P. H. Aubert, P. Audebert, M. Roche, P. Capdevielle, M. Maumy and G. Ricart, *Chem. Mater.*, 2001, **13**, 2223–2230.
19 S. Curreli, E. C. Escudero-Adan, J. Benet-Buchholz and A. W. Kleij, *Eur. J. Inorg. Chem.*, 2008, 2863–2873.
20 G. Venkatachalam, N. Raja, D. Pandiarajan and R. Ramesh, *Spectrochim. Acta, Part A*, 2008, **71**, 884–891.
21 H. Byrd, C. E. Holloway, J. Pogue, S. Kircus, R. C. Advincula and W. Knoll, *Langmuir*, 2000, **16**, 10322–10328.

22 K. Martinusz, E. Czirok and G. Inzelt, *J. Electroanal. Chem.*, 1994, **379**, 437–444.

23 K. C. Gupta and A. K. Sutar, *React. Funct. Polym.*, 2008, **68**, 12–26.

24 F. Bedioui, E. Labbe, S. Gutierrezgranados and J. Devynck, *J. Electroanal. Chem.*, 1991, **301**, 267–274.

25 K. D. Izutsu, *Electrochemistry in nonaqueous solutions*, Wiley-VCH, Weinheim, 2nd, rev. andenlarged edn, 2009.

26 M. VilasBoas, C. Freire, B. deCastro, P. A. Christensen and A. R. Hillman, *Inorg. Chem.*, 1997, **36**, 4919–4929.

27 J. L. Li, F. Gao, Y. K. Zhang, L. Z. He, G. M. Han and X. D. Wang, *Acta Phys.-Chim. Sin.*, 2010, **26**, 2647–2652.

28 D. E. Richardson and H. Taube, *Inorg. Chem.*, 1981, **20**, 1278–1285.

29 D. E. Richardson and H. Taube, *Coord. Chem. Rev.*, 1984, **60**, 107–129.

30 F. N. Rein, R. C. Rocha and H. E. Toma, *Electrochem. Commun.*, 2002, **4**, 436–441.

31 P. Day, *Recherche*, 1981, **12**, 304–311.

32 A. S. Lima, N. Bocchi, H. M. Gomes and M. F. S. Teixeira, *Sensors*, 2009, **9**, 6613–6625.

33 Y. Marcus, *Chem. Rev.*, 1988, **88**, 1475–1498.

34 A. A. El-Shafei, *J. Electroanal. Chem.*, 1999, **471**, 89–95.

35 D. Lin-Vien, *The handbook of infrared and Raman characteristic frequencies of organic molecules*, Academic Press, Boston, 1991.